

GROUND TRUTH LOCATION USING A SYNERGY BETWEEN INSAR AND SEISMIC METHODS

Chandan K. Saikia¹, Rowena Lohman², Gene Ichinose¹ and Mark Simons²

URS Group, Inc.;¹ California Institute of Technology²

Sponsored by Air Force Research Laboratory

Contract No. DTRA01-01-C-0072

ABSTRACT

The objective of this study is to utilize Synthetic Aperture Radar Interferometry (InSAR) to estimate accurate hypocenter locations for shallow and moderate-sized earthquakes in the Middle East and Eastern Asia. We have acquired different levels of Digital Terrain Elevation Data (DTED) from National Imagery and Mapping Agency for this region to improve the InSAR processing. Once surface deformation is identified in the InSAR signal and associated with an earthquake, the hypocenter location is estimated from a combination of geodetic and seismic modeling to provide accurate locations for regional velocity model calibration. One primary difficulty in the analysis of InSAR is the uncertainty in hypocenter location with the increasing earthquake size because of the increase of fault area with seismic moment. Another difficulty is the trade-off between fault area and fault slip and between focal mechanism and location because InSAR only measures the 3-components of surface deformation along a line of sight (e.g., Lohman et al., 2002).

Saikia et al. (2002) combined InSAR and seismic data modeling to estimate the location of the 1999/04/30 M_w 4.8 earthquake in Southern Iran. The focal depth is 4 km, which was estimated from modeling InSAR data. When we compared the Lg-waves at station RAYN between this event and a nearby 1998/11/13 earthquake (depth=9 km), the Lg-wave characteristics were similar indicating that both are shallow depth earthquakes. We performed a grid-search and inversion of the regional long-period waveforms and high-frequency P-waves to reaffirm this earthquake's shallow depth and help constrain the focal mechanism estimated from InSAR modeling. Using the accurate hypocenter location estimated from InSAR and seismic waveform modeling (probably now GT1), we obtained empirical SSSCs at regional stations between (0-30°) and relocated 11 other earthquakes ($4.4 < m_b < 5.7$) that occurred near this event. The SSSC significantly reduced the area of the error ellipse for these earthquakes.

In this study, we used InSAR data to examine additional events in Southern Iran. We examined the 1998/10/18 (m_b 4.2), 1997/05/05 (m_b 4.8), 1997/09/18 (m_b 4.7), and 1999/04/28 (m_b 4.8) earthquakes. The satellite radar data available for these events spanned a time interval that included several events making the association of the observed deformation field with each earthquake difficult. For example, radar data for events of 1997/05/05 and 1997/09/18 were obtained from track 478 /frame 3069, which spanned a time interval between April 1996 and April 1999. During this time interval, several events occurred within 50-80 km of the identified SAR signal locations. However, based on InSAR analysis, most of these events did not contribute to the radar signal as they were too small ($m_b < 4.5$). Broadband waveforms from station RAYN were compiled for all events occurring during each time interval of the radar data and investigated for their high-frequency Lg-wave characteristics. We also modeled the teleseismic and regional P-waves and long-period waveforms. The following are a list of conclusions: 1). processing and modeling of InSAR data identifies four shallow earthquakes, 2). within the limits of resolution, seismic depths determined from the modeling of the long-period seismic waveform and far-regional broadband P waveforms are consistent with the depths determined by modeling the InSAR ground deformation, 3). the ISC depths are often poorly estimated, and 4). locations of small seismic events improve, when the SSSCs estimated using the location of events determined from the synergy of InSAR and seismic are applied during location.

OBJECTIVES

The goal of this ongoing study is to obtain reliable locations for moderate-sized earthquakes ($M_w < 5.5$) in parts of Asia and Middle East. We will deliver accurate locations, associated waveforms, raw satellite synthetic radar interferometry (InSAR) images, processed InSAR phase maps and ground deformation maps to the Department of Energy knowledge database.

The study is divided into two parts: seismic and geodetic, which are concerned with identifying ground truth (GT) locations for reference events in regions of monitoring interest. The primary objective is to improve earthquake locations to within the GT10 or GT5 level of accuracy (i.e., events within 10 or 5 km accuracy in their epicentral locations, respectively) when they apparently satisfy the GT25 criteria (Yang and Romney, 1999). The other objective is to utilize geodetic data, including synthetic aperture radar interferometry (InSAR) to establish accurate locations for shallow and moderate-sized seismic events ($M_w < 5.2$) to validate the ground truth (GT) results determined from seismic methods.

The final task of this study combines seismic and geodetic results to validate the GT locations. These locations determined from InSAR will be used to develop station-specific-source corrections (SSSCs) for the upper-mantle P-wave phase arrivals, which in turn will be used for relocating nearby earthquakes ($M_w < 4.5$).

RESEARCH ACCOMPLISHED

1999/04/30 Event

Radar images have been used by many authors to identify surface deformation generated by earthquakes and mine collapses in many parts of the world (Feigl *et al.*, 1995; Massonnet and Feigl, 1998; Foxall *et al.*, 1998; Akoi *et al.*, 1999; Rigo and Massonnet, 1999, Stromondo *et al.*, 1999; Myers *et al.*, 2002; Steck *et al.*, 2002; Lohman *et al.*, 2002). Saikia *et al.* (2002) studied a small earthquake that occurred in southern Iran on April 30, 1999 (M_w 4.8) and estimated its location by modeling the ground deformation identified from a geocoded interferograms (Figure 1), formed using radar images for track 20/frame 3051 (99/04/21-99/05-26) and for track 249./frame 3051 (99/04/02-99/06/11), respectively. The radar images were processed by removing topography, filtering and unwrapping of the phase. Topography was removed by using digital elevation model (DEM) from the level 1 Digital Terrain Elevation Data (DTED). In Figure 1, the surface deformation generated by this earthquake is observed in the upper right of the image at location of 27.87°N and 53.610°E as two circular interferometric fringes. In our earlier report, we estimated a hypocentral depth of less than 9 km based the characteristics of high frequency ($f > 1$ Hz) Lg-waves. These Lg-waves generated by this earthquake were compared to a co-located earthquake on November 13, 1998 (depth < 9 km) at a broadband station RAYN in Saudi Arabia ($\Delta=938$ km, $AZ=241^\circ$). By modeling the deformation determined from the InSAR images, we estimated its depth at 4 km. We also inverted for the centroid moment tensor using long-period regional-waves recorded at stations RAYN, GNI ($\Delta=1591$ km, azimuth=332°) and ATD ($\Delta=2126$ km, $AZ=214^\circ$). Within the limits of resolution of the long-period waves, the centroid depth is resolved to within 2 to 10 km (Figure 2). The focal depth of 35 km, estimated by ISC, using the P travel times only, is poorly determined. Further, forward modeling of the broadband P wave displacements at stations ATD and KIV ($\Delta=18.3^\circ$) also yielded the hypocentral depth less than 5 km. In Figure 3, we present the move-out of pP and sP depth phases relative to the P onset. Both ATD and KIV are located within the range of upper-mantle discontinuity triplications but the modeling and data indicate that the depth phases have not separated from the P-wave onsets. Synthetics generated at a depth of 4 km show the best agreement with the recorded waveform. Table 1 presented in Saikia *et al.* (2002) shows a comparison of various locations that were available for this earthquake including the one determined using the synergy of the InSAR (epicentral location) and seismic data (depth and travel times of P waves). This way, we predict the most reliable origin time for this event. Note that the other locations are biased and the HRV (Harvard) location is the worst.

We used the location of the April 30, 1999 earthquake estimated by the synergy of InSAR and seismic methods to estimate Source Specific Station Corrections (SSSCs) for regional and teleseismic stations. About 11 other events occurred in the proximity of this earthquake. We applied these SSSCs and relocated these earthquakes (Table 2.). The applications of the empirical SSSCs have reduced the ellipse error area for seven events (based on the error ellipse estimated at a 90% confidence interval). The 1998/07/01 earthquake (m_b 3.9) and had a large azimuthal gap of 112° for its recording stations. With the application of the SSSCs, its error ellipse area has significantly

increased, but the error ellipse area decreased for events when the azimuthal gap was less than 35°.

Table 1. Location Parameters for 1999/04/30 Southern Iran Earthquake

Date d/m/y	Origin Time hr:mn:ss	Latitude (°N)	Longitude (°E)	Z (km)	ΔR (km)	Agency
04/30/99		27.870	53.610			INSAR
04/30/99	04:20:02.0	27.765	53.519	33.1	14.68	ISC (MOS)
04/30/99	04:20:22.5	27.837	53.538	35.0	7.0	USGS
04/30/99	04:19:59.6	27.748	53.553	4.0 (F)	14.6	URS
04/30/99	04:20:05.4	27.866	53.576	45.0	3.04	URS
04/30/99	04:20:12.5	27.74	52.960	44.9	65.65	HRV
04/30/99	04:20:00.1	27.870 (F)	53.610 (F)	4.0 (F)		Seis+INSAR

(F) - Fixed location or depth

Table 2. Relocation of Southern Iran earthquakes using 1999/04/30 as the Reference Event

Date	h:m:s	°N	°E	Z (km)	m_b	Gap	# Sta	ER(1)	ER(2)
96/05/24	06:35:56.30	27.80	53.576	3.3	4.4	28	162	38.3	25.61
96/05/25	17:00:54.70	27.82	53.554	3.2	4.8	40	109	32.2	30.43
98/06/13	02:23:42.70	27.86	53.745	8.3	4.6	45	102	32.5	45.99
98/07/01	21:36:31.70	27.79	53.688	12	3.9	112	12	1344.2	1632.5
98/11/13	13:01:07.80	27.75	53.672	2.8	5.3	28	257	14.4	11.59
98/11/14	10:37:20.50	27.89	53.633	10	4.6	42	102	51.2	75.58
98/12/10	14:21:49.80	27.89	53.581	10	4.7	63	98	39.9	58.23
98/12/27	04:10:39.30	27.84	53.688	8.9	4.7	63	116	42.1	32.51
99/04/28	18:11:41.50	27.83	53.595	3.9	4.5	34	134	34.4	25.32
99/05/06	23:00:50.20	29.49	51.971	3.3	5.7	28	289	32.2	8.41
99/05/06	23:13:24.40	29.57	51.954	10	5.2	35	217	27.1	42.96

(ER1) minor axis length of error ellipse, (ER2) major axis length of error ellipse

1997/05/05 and 1997/09/18 Events

We then examined the availability of the radar data for nearly 200 events in southern Iran. We requested radar data for 90 events from the European Space Agency based on the time span and baseline criteria. These events included mostly smaller magnitude earthquakes, and since the ISC depths and locations are often unreliable for such magnitudes, we decided to obtain waveform data for additional analysis. For example, Figure 4 shows a set of vertical component velocity seismograms recorded from many earthquakes in our study area in the magnitude range of $3.9 < m_b < 4.9$. These seismograms are all recorded at station RAYN from earthquakes nearly co-located at approximately 938 km to the northeast. The seismograms were filtered to frequencies above 1 Hz in order to examine their Lg-wave characteristics. The best characteristic of Lg-waves is their extended durations with decreasing focal depth. For each seismogram, we labeled the origin time (hour:min), peak amplitude (in counts), ISC magnitude (m_b) and ISC depth (km). In these waveforms, not only the Lg-waves, but also the onsets of the P waves are quite clear. We infer from the extended duration of the Lg-waves that these events have shallow depths.

Figure 5a shows interferograms constructed using radar data acquired from track 478/frame 3069 spanning the time period from April 1996 to April 1999 where signals for two events can be identified at 27.1345°N, 53.8842°E and 27.0886°N and 53.9412°E. The northern most deformation (event-N) has a lobe of subsidence and uplift, which is adjacent to and superimposed upon a smaller lobe of uplift (event-S). Modeling these deformations observed in the InSAR signal required two events at depths of 5.6 and 4 km with focal mechanism of $\delta=3^\circ$, $\lambda=90^\circ$, $\phi=309^\circ$ and $\delta=60^\circ$, $\lambda=90^\circ$, $\phi=280^\circ$ respectively (Figure 5b). We used Okada's (1992) formulation to compute three-component surface deformation at each grid point, rotated them along the line of sight (LOS) and multiplied by the LOS directional cosines used in processing the interferogram (Figure 5a). Modeling and fit was performed using Neighborhood Algorithm developed by Sambridge (1998). Figure 5c shows the residual between the observed and synthetic surface deformations.

By examining the ISC bulletins, we identified 22 events that occurred within 50 km of the first InSAR signal. Majority of these events have large location uncertainties because they were located using P-wave travel-times from only a sparse distribution of seismic stations, mostly beyond 10° (e.g., 2-3 stations within 6°), which does not provide an adequate azimuthal coverage. Of these, one event, which occurred on 1997/05/05 (15h:11m, m_b 4.8), is within 2 km of this InSAR signal. This earthquake was reported by 220 stations ($\Delta \geq 9.5^\circ$) providing an azimuthal gap of 71° . According to the ISC, the 1997/05/05 event occurred at a depth of 47.5 ± 9.4 km. The Harvard Centroid Moment Tensor catalog (HRV) lists a depth of 15 km with an M_w of 5.1.

We applied waveform modeling and inversion to estimate the centroid depth and focal mechanism for the 1997/05/05 and 1997/09/18 earthquakes. We inverted long-period regional waveforms recorded at RAYN to estimate the focal mechanism and centroid depth (Figure 6a) of event 1997/05/05. The source parameters for nodal plane #1 are $\delta=69^\circ$, $\lambda=123^\circ$, $\phi=336^\circ$, $M_w=4.94$, $z=16$ km, which is different from the HRV solution for the most similar nodal plane ($\delta=52^\circ$, $\lambda=128^\circ$, $\phi=296^\circ$, $M_w=5.1$). The centroid depth of 16 km is poorly resolved from the long-period regional-waves from a single station. For a better estimate and resolution of the centroid depth, we examined broadband regional P-waves. Using our focal mechanism, a suite of $f-k$ synthetics were computed for stations ATD and KIV at depths ranging between 2 and 10 km in 2 km increments. The synthetics were compared them with the recorded P-waves. Based on this additional analysis, we found the depth of this event is shallower than 6 km.

A second event also occurred at a distance of 4.72 km from this InSAR signal on 1997/09/18 (m_b 4.7-5.2). This event was recorded by 184 stations globally with an azimuthal gap of 64° . We performed a moment tensor inversion on the long-period regional-waves recorded at stations RAYN, ABKT and GNI. We estimated source parameters of (Nodal Plane 1: $\delta=19^\circ$, $\lambda=89^\circ$, $\phi=110^\circ$), (Nodal Plane 2: $\delta=71^\circ$, $\lambda=90^\circ$, $\phi=292^\circ$) and ($M_w=4.7-5.1$, $z=2-8$ km). The ISC reported a depth at 55 km, but long-period modeling of recorded seismograms at these stations yielded its depth at 2-8 km (Figure 6b). The broadband regional P waveform at ATD indicates a shallow depth (about 2-4 km). A comparison of the Lg-waves in Figure 4 also indicated that these earthquakes are shallow. Note that both these events are located at 5.7 and 4.6 km from the second InSAR location in the interferogram (Figure 5). The 1997/09/18 event was reported by 181 stations, which provided an azimuthal gap of 71° , but lacked P-wave travel times from local stations. We can associate the 1997/05/05 event to the first InSAR signal because of its close proximity of the ISC location to the centroid location based on the modeling of the InSAR signal. The 1997/09/18 event is probably the second InSAR signal, as there is no occurrence of any other seismic events within this vicinity, which can contribute to the InSAR deformation signal.

Figure 7 shows an interferogram constructed from radar data acquired from track 13/frame 567 (time span between October 1997 and September 1999) which shows range deformation of about 1 cm at 28.6736°N , 54.2484°E . We were able to identify this event on multiple interferograms, thus reducing the possibility that it was caused by other sources of errors. During the time span between 10/97 and 9/99, 14 earthquakes with magnitudes (m_b) between 3.9 and 4.7 occurred within 100 km of this InSAR signal. Of these, two events on October 18, 1998 (28.5848°N , 54.2007°E ; m_b 4.2) and on October 19, 1998 (28.4764°N , 54.4519°E ; m_b 3.9) occurred within 50 km. Of the two events, the event of the 18th occurred 11 km from the location of InSAR signal. According to the ISC bulletin, the depth of this event is at 97.7 km and it is reported to have damaged sixty houses in Darab area, which is unlikely for an event of this size at such depth. The slightly smaller second event ($m_b < 3.9$) occurred about 29.5 km away along the southeast direction from the InSAR signal. It is too small of an event in magnitude to contribute to the InSAR signal.

CONCLUSIONS AND RECOMMENDATIONS

Estimating accurate ground truth locations for earthquakes is difficult in areas where seismic network stations are sparse or inaccessible. The addition of InSAR data can overcome this difficulty and provide accurate ground truth locations. Earthquakes that do not produce surface rupture may still generate measurable surface deformation observed from processed radar images acquired before and after the event. However, atmospheric noise or topographical uncertainty may have a correlation length smaller than the regular coherence estimation window, which may prevent retrieval of useful InSAR signals from processed interferograms. Nevertheless, when ground deformation is identified in interferograms, hypocenter locations of seismic events can be reliably estimated within the error of the fault dimensions (for M 5 earthquake this is about 1-2 km).

We have noted that events, which produced identifiable ground deformation within the Zagros of southern Iran, are estimated to have occurred at depths less than 15 km. Hypocenter depths estimated by ISC and HRV, which ranged from 15 to 90 km, are poorly resolved based on combined InSAR and seismic source depth modeling estimates. Moment tensor inversion or long-period regional-waves and broadband regional P-waves are more consistent with InSAR modeling (less than 6 to 10 km). Since the depths for many earthquakes in this region are mostly overestimated, then it is encouraging from the viewpoint that many deeper events may be suitable for this type of analysis. Since acquiring radar data is expensive, it is therefore necessary to assess their depths by carefully modeling the regional-wave long-period waveforms and regional broadband P-waves, especially the interaction of P with pP or sP depth phases recorded at regional station as we have demonstrated in Figure 6.

The following are a list of conclusions: 1). processing and modeling of InSAR data identifies four shallow earthquakes, 2). within the limits of resolution, seismic depths determined from the modeling of the long-period seismic waveform and far-regional broadband P waveforms are consistent with the depths determined by modeling the InSAR ground deformation, 3). the ISC depths are often poorly estimated, and 4). locations of small seismic events improve, when the SSSCs estimated using the location of events determined from the synergy of InSAR and seismic are applied during location.

In our continuing effort to improve radar data processing, we have acquired Digital Terrain Elevation Data (DTED) for different levels (e.g., from highest to lowest resolution: level 0, 1, and 2) to form high-resolution digital elevation models in countries including China, India, Pakistan, Afghanistan, Iran, Iraq, and Saudi Arabia. We applied DTED level 1 data in processing of radar data, which have greatly improved our processing capability. We found that the time span between the scenes of the pre- and post-seismic deformation must be small. Otherwise, several earthquakes may occur within the time span, as is the case in our investigation, which can contribute to the ground deformation that is discernable in the interferogram. In such situations, associating of a seismic event to the observed ground deformation becomes difficult.

The surface deformation caused by large earthquakes ($M > 6$) is of limited significance because the large source size makes it difficult to associate the observed deformation to a definite source rupture initiation (i.e., the hypocenter). The ambiguity between the location of surface deformation and epicenter location is reduced significantly for smaller magnitude earthquake. Because of the offset between locations of surface deformation and epicentral locations, ground deformation discernable in the differential InSAR must be analyzed in conjunction with the seismic data that can provide focal mechanism and event depth. It is also essential to perform error analysis to some degree of confidence limits of the epicentral locations.

REFERENCE

- Akoi, S., M. Furuya, S. Kobayashi and S. Okubo (2002). Co-seismic crustal deformation of the 1996 Onikobe earthquakes, Japan, detected by InSAR, *Eos. Trans. AGU* 83(47), Fall Meeting Suppl. Abs G61B-0994.
- Feigl, K. L., A. Sergent, and D. Jacq (1995). Estimation of an earthquake focal mechanism from satellite interferogram: Application to December 4, 1992 Landers aftershock, *Geophys. Res. Lett.* 9, 1037-104.
- Foxall, B., J. J. Sweeny, and W. R. Walter (1998). Identification of mine collapses, explosions and earthquakes using InSAR: a preliminary investigation, in *Proceed. 20th Annual Seismic Res. Symposium., Monitoring Comprehensive Test Ban Treaty*, 21-23 September, 408-416.
- Lohman, R. B., M. Simons and B. Savage (2002). Location and mechanism of the Little Skull Mountain earthquake as constrained by satellite radar interferometry and seismic waveform modeling, *J. Geophys. Res.*, 107, 10.1029/2001JB000627. ETG, 7-1 to 7-8.
- Massonnet, D. and K. L. Feigl (1998). Radar interferometry and its application top changes in the Earth's surface , *Rev. Geophys.*, Vol 36, No. 4, 441-500.
- Myers, S., M. Flanagan, M. Pasyanos, W. Walter, P. Vincent and C. Shultz (2002). Location calibration in western Eurasia and North Africa: Ground truth improved earth models, Bayesian Kriging, regional analysis, location algorithms, array calibration and validation, *24th Seism. Res. Rev., Nuclear Explosion Monitoring: Innovation and Integration*, Sept 17-19, 351-360.
- Okada, Y. (1992). Internal deformation due to shear and tensile faults in a half-space, *Bull. Seism. Soc. Am.* 82, 1018-1040.
- Rigo, A. and D. Massonnet (1999). Investigating the 1996 Pyrenean earthquake (France) with SAR interferograms heavily distorted by atmosphere, *Geophys. Res. Lett.*, 26, 3217-3220.

- Saikia, C. K., R. Lohman, G. Ichinose, D. Helmberger, M. Simons and P. Rosen (2002). Ground truth locations - A synergy of Seismic and Synthetic Aperture Radar Interferometric Methods, 24th Seism. Res. Rev., Nuclear Explosion Monitoring: Innovation and Integration, Sept 17-19, p420-429.
- Sambridge, M. (1998). Geophysical inversion with a neighborhood algorithm - I, Searching a parameter space, Geophys. J. Int. 138, 479-494.
- Steck, L. H. Hartse, C. Bradley, C. Aprea, A. Valesco, G. Randall, and J. Franks (2002). Regional location calibration in Asia, 24th Seism. Res. Rev., Nuclear Explosion Monitoring: Innovation and Integration, Sept 17-19,, p430-439.
- Stramondo, S., M. Tesauro, P. Briole, E. Sansosti, S. Salvi, R. Lanari, M. Anzidei, P. Baldi, G. Fornaro, A. Avallone, M. Buongiorno, G. Franceschetti, E. Boschi (1999). The September 26, 1997 Colfritro, Italy earthquakes: modeled coseismic surface displacement from SAR interferometry and GPS, Geophys. Res. Lett, 26. 883-886.
- Yang, X. and C. Romney (1999). PIDC ground truth event (GT) database (revision 1), CMR Tech Rept, CMR-00/15.

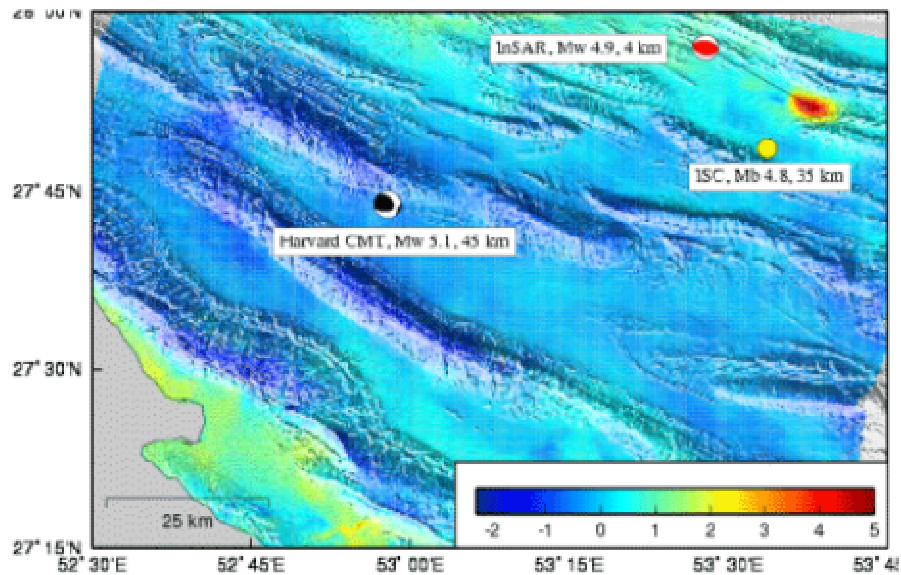


Figure 1. LOS displacement field from interferogram constructed from scenes acquired between 1999/04/21 and 1999/05/26. There is a lobe of uplift of about 5 cm observed in the InSAR that was modeled to estimate the focal mechanism shown in the upper-right. The ISC location for the 1999/04/30 event is shown and associated with this deformation. The thrust mechanism of the Harvard centroid moment tensor is consistent with the InSAR modeling yet the hypocenter and centroid depth for both ISC and HRV locations are in error by about 30 to 40 km.

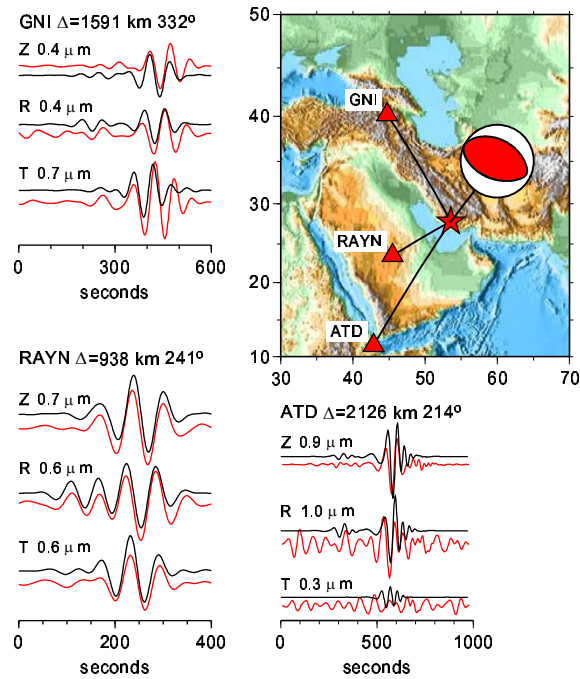


Figure 2. Observed and predicted regional-waves filtered to long-periods (100-50 sec) for the 1999/04/30 04:20 UTC event. The observed seismograms were used to invert for the Moment tensor.

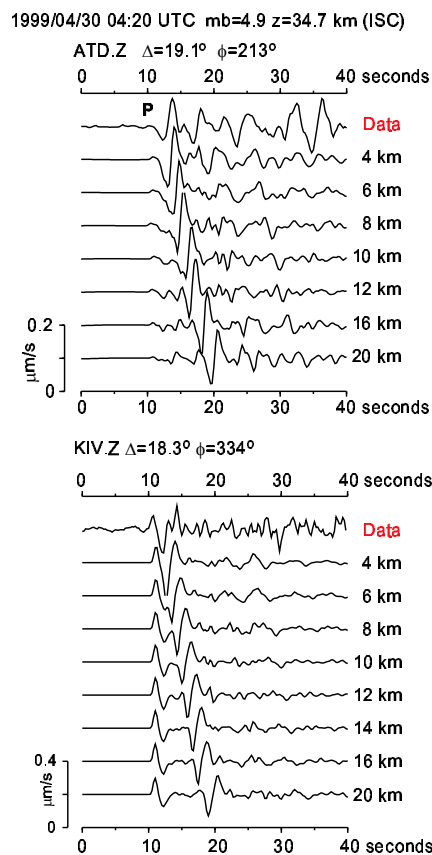


Figure 3. Modeling broadband far-regional P-waves for the 1999/04/30 04:20 UTC event. The P-waves from stations ATD and KIV are aligned and compared to synthetics computed at 2 km depth increments.

The depth phases and upper-mantle phases indicate that this event has a shallow depth of less than 6 km. We used the source parameters estimated from the long-period moment tensor inversion (Figure 2) to compute the synthetics.

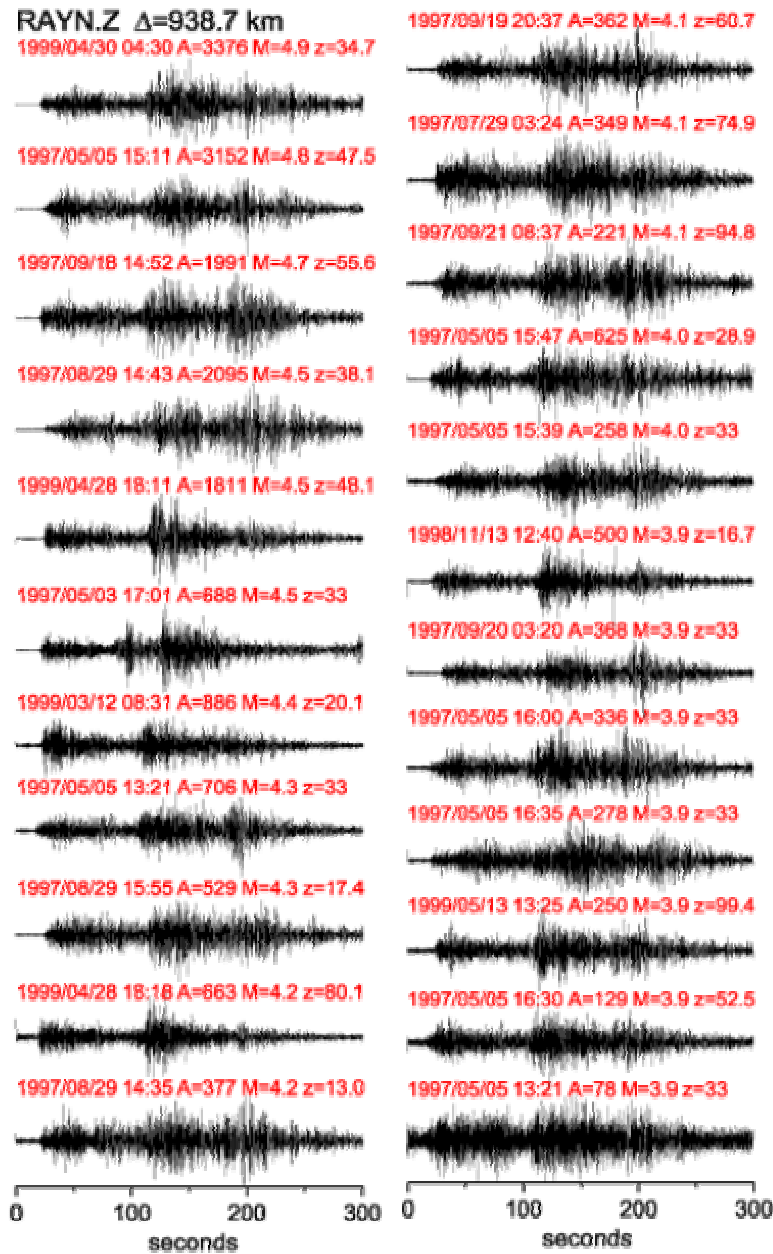


Figure 4. RAYN vertical component velocity seismograms high-pass filtered at 1 Hz.

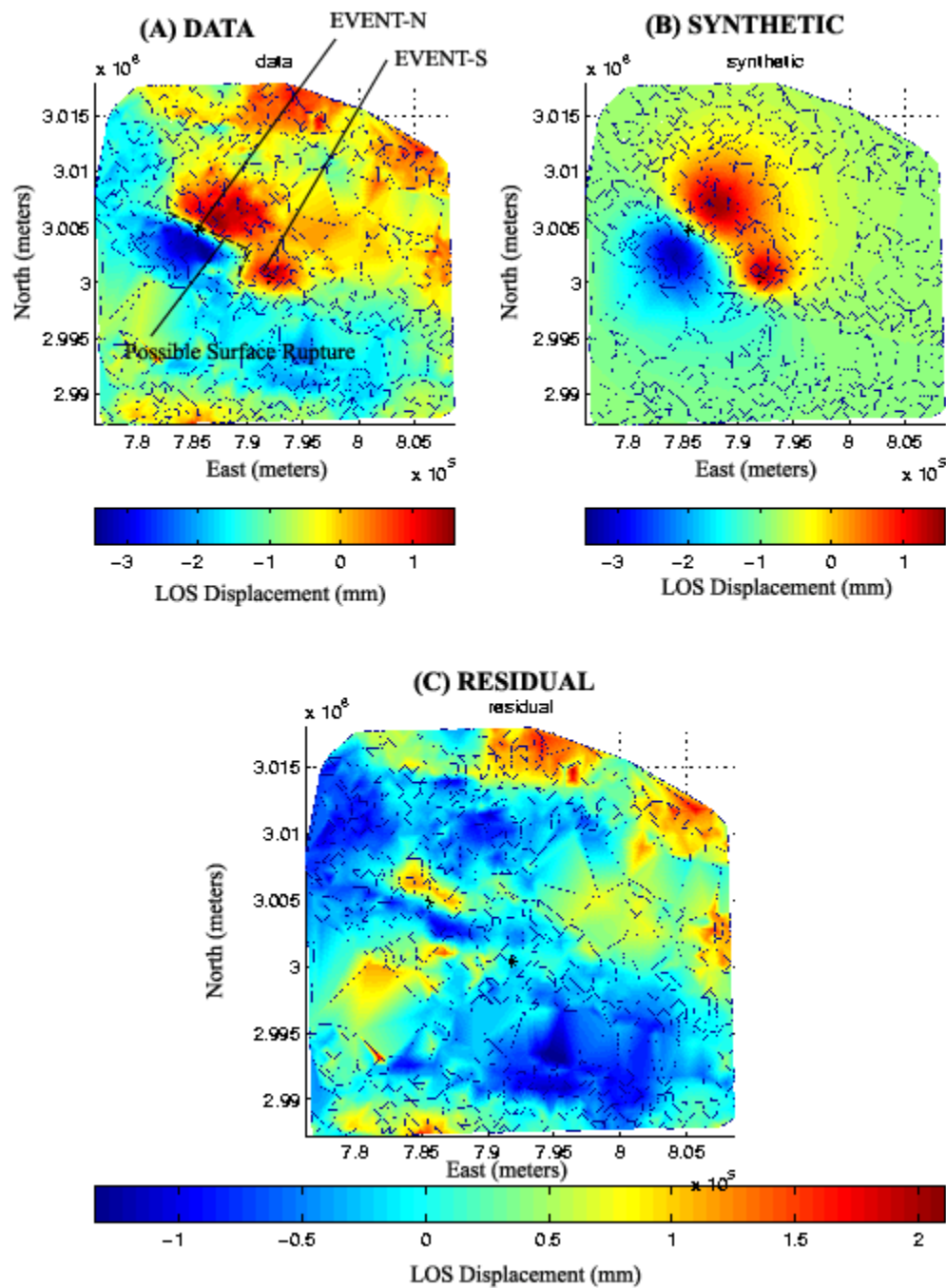


Figure 5 (a) observed InSAR Interferogram for event-N (1997/09/18) and event-S (1997/05/05), (b) synthetic surface displacements estimated from a grid-search inversion, and (c) residuals between observed and synthetics.

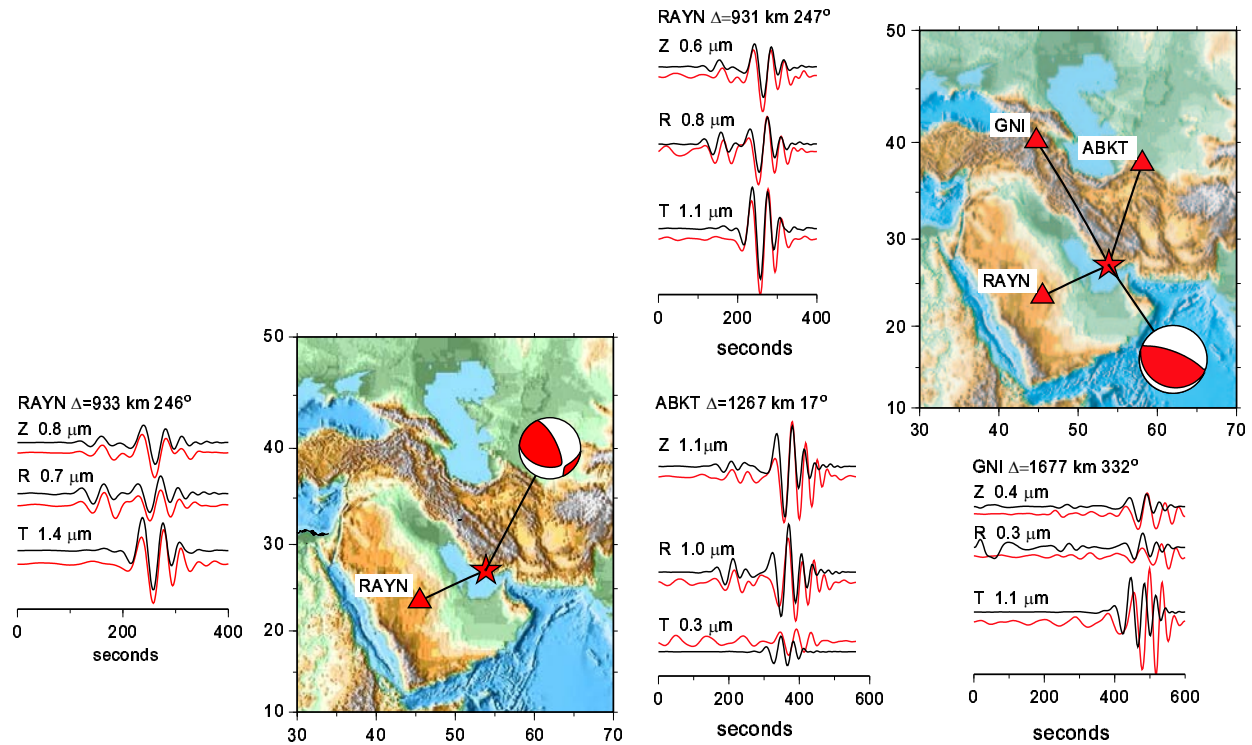


Figure 6. (A-Left) Regional-wave moment tensor inversion results for event 1997/05/05. (B-right) Regional-wave moment tensor inversion results for event 1997/09/18.

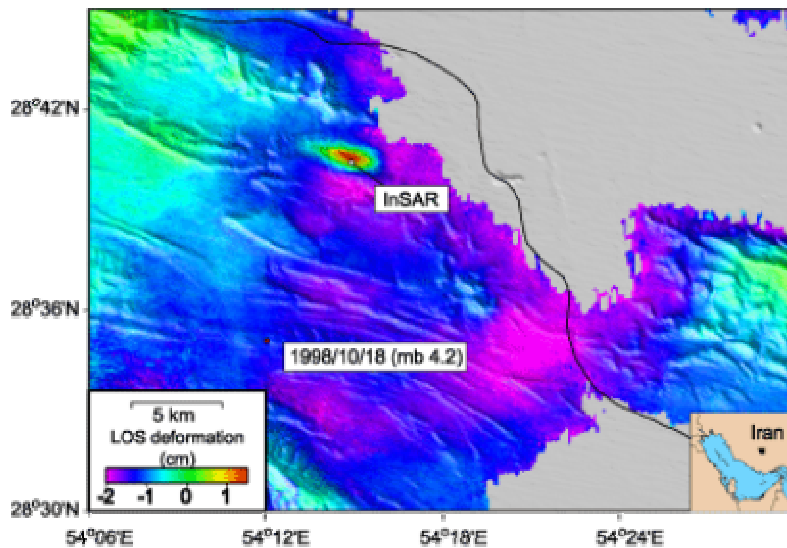


Figure 7. LOS displacement field from interferogram constructed from scenes acquired between 1997/10 and 1999/09 that a peak deformation of about 1 cm at 28.6736°N, 54.2484°E. This deformation may be associate with the 1998/10/18 event that the ISC estimates at mb 4.2. Unfortunately, to our knowledge, there is no available seismic waveform data for this event at stations RAYN or ATD for this date.